

Dynamic Analysis of Airflow Features in a 3D Real-Anatomical Geometry of the Human Nasal Cavity

H. Tang¹, J.Y. Tu¹, H.F. Li¹, B. Au-Hijleh¹, C.C. Xue², C.G. Li²

¹School of Aerospace, Mechanical & Manufacturing Engineering

²School of Health Sciences

RMIT University, Melbourne, VIC, 3083 AUSTRALIA

Abstract

Drug delivery in the human respiratory tract is a long standing challenge due to the complexity of the geometry and materials properties. This paper presents a brief summary of flow features in the human respiratory system and simulates an airflow field based on a 3D real-anatomical geometry of the human nasal cavity. A Lagrangian particle-tracking approach is adopted in the flow field solver for the dispersed phase. The dispersion characteristics of particles through the airflow are investigated under the quiet breathing. The particles passing through the domain sections for different value of particle density, diameter and flow rate are investigated. The particle deposition efficiency is also studied. These were compared with experimental data, and results of previous simulations. It is noted that the transportation, dispersion and deposition of particles can be controlled by the particle properties and flow rate. The numerical results show good agreement with previous experimental and computational studies, which are useful for the optimisation design of therapy methodologies, treatment devices and drug materials.

Introduction

Drug delivery in the human respiratory tract is a long standing challenge due to the complexity of the geometry and materials properties. Inhaling micronized drugs is highly effective and convenient. Information on the velocity distribution and local concentration of solid particle is very important in the design of inhalers that deliver the drugs into lung airways. Scaled-up laboratory models can be used to study the flows in the human respiratory tract; however, the time consuming and expensive nature of experiments carried out in this area mean that computational studies of the processes taking place will become more important. Furthermore, numerical analysis allows investigators to “test” various models under different conditions in relatively short time and at reduced cost. For the past decade, advancements in computational models employing the Computational Fluid Dynamics (CFD) techniques have emerged from the simultaneous modelling of the airflow field distribution, particle trajectory and deposition in human airways. Some of the notable works are: Balashazy and Hofmann [1], Yu *et al.* [2], Zhang *et al.* [3, 4], Martonen *et al.* [5], Gemci *et al.* [6] and Matida *et al.* [7]. In parallel with these computational efforts, a number of important experimental works on particle deposition in the human airways have also been performed, for example, Hahn *et al.* [8], Swift and Strong [9] and Hörschler *et al.* [10].

The nose is a major component of the human respiratory system and also performs important functions in drug delivery. In this paper, we present a brief summary of flow features in the human respiratory system and simulate an airflow field based on a 3D real-anatomical geometry of the human nasal cavity. A Lagrangian stochastic particle-tracking approach is adopted in the flow field solver for the particle dispersion and continuous phases. The dispersion characteristics of particles through the airflow are investigated under the quiet breathing. The particles

passing through the sampling planes for different value of particle density, diameter and flow rate are investigated.

Fluid Dynamic Perspective of the Human Respiratory System

Flow Features

The flow features of the airway in the human respiratory system are extremely complex, involving characteristics of multiple-phase flows in laminar, turbulent and interactive conditions as summarized in Table 1.

A solo simulation approach is difficult to cover all flow features as shown in table 1. Therefore, what’s simulation approaches should be taken is depend on main concerns of investigation; physical model was established on a simplified concept and coupled with suitable mathematic algorithms. However, the computational domain should be close to the real-anatomical geometry in order to capture real flow feature. It is worth emphasizing that the geometry of the nasal cavity is a major determination factor of the particle deposition pattern and airflow field.

Anatomical Geometry and Computational Domain

The nasal cavity is a complex structure as shown in Figure 1, an anatomical illustration of a left nasal cavity of adult. A 3D real-anatomical geometry reconstructed from a CT fine-scanned data is shown on Figure 2. The surface of this real nasal cavity has complex boundary features, is desirable for the investigation. However, numerous detail boundary features result in hung mesh grids and computation time consuming leading to impracticable at this stage.

An anatomically corrected model of an adult nose was used as a computational domain in present study as shown in Figure 3. It is reconstructed from a CT scanned data via CAD solid model design software, but has been smoothed due to less slice data. This model was developed originally by Prof. Scherer and his bioengineering research group at the Department of Bioengineering, University of Pennsylvania and used in several of their published works [7, 11, 12] and further improved on mesh construction by present study.

Flow Configuration

The range of computational domain is shown in blue coloured area of the anatomical illustration in Figure 1. The model of computational domain is shown in Figure 3. The domain is divided into 9 sections.

The airflow rate \forall is corresponding to normal quiet breathing for a single nostril. Laminar flow is simulated. Drug delivery is assumed to be particulate flow with a uniform diameter D_p from 1~40 μ m, particle density ρ_p is varied from 500 kg/m³ to 2000 kg/m³.

Breathing conditions		Behaviour & Symptoms	Related locations	Main flow features	Simulation approaches
1	Normal: -quiet -resting -sleeping	Inspiration Expiration Flow rate of 125-200 ml/s	a. nasal cavity b. larynx c. trachea d. bronchi	Periodic flow, Laminar flow, Gap flow, small deformation at the junction of b and c.	sinusoidal velocity profiles, single phase approach
2	Abnormal: -exertion -sickness -physical exercise	-asthma -nasal polyp -heavy vibrissae -foreign-body -sneezing Flow rate of 200-625 ml/s		constriction flow, obstruction flow, extra mucus flow, high flow rate, turbulent flow, deformation at the junction of a to d.	single phase approach, multiphase approach, turbulent model free surface model, Fluid-Structure Interaction (FSI) approach,
		-morbid surface	excessive dry/secretion of the mucosal surface permeation flow	liquid film flow model specific boundary model porous media model	
3	Drug delivery: -inhaler -collunarium	Therapy spray	a. nasal cavity b. larynx c. trachea d. bronchi	high flow rate with deformations and vibrations in c or d-e	FSI approach, acoustic approach
4	Air pollutions: -dust air: inorganic dust, organic dust, synthetic material dust -chemical gas	Silicosis Asbestosis chronic obstructive pulmonary diseases, COPD			

Table 1. Fluid dynamic perspective of the human respiratory

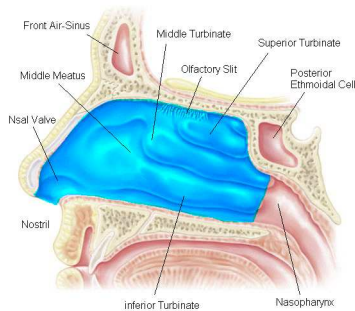


Figure 1. An anatomical illustration of left nasal cavity, shaded (blue) area show the range of computational domain in present study.

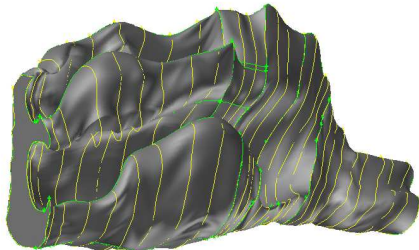


Figure 2. A 3D real-anatomical geometry reconstructed from CT fine-scanned data show the complex boundary details.

The particle deposition is defined in term of Local Particle Deposition efficiency (LPD) = ((number of particles entering the section n)-[number of particles exiting section n])/ number of

particles entering section n , and Total Particle Deposition efficiency (TPD) = ((number of particles entering the domain)

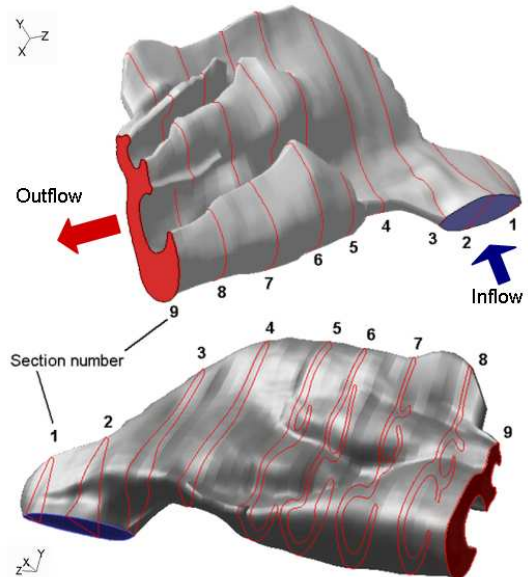


Figure 3. Computational domain is an anatomically corrected model of an adult nose built from CT slice data.

-[number of particles exiting section 9])/ number of particles entering section 9. Stokes number St_{Amin} is defined:

$$St_{Amin} \equiv \frac{\pi^{0.5} d_a \forall}{18 \mu A_{min}^{1.5}}, \quad d_a \equiv D_p \sqrt{\frac{\rho_p}{\rho_0}}, \quad \text{where } d_a \text{ is the aerodynamic diameter and is a function of the particle diameter and density.}$$

The particle density is normalized by the reference density (ρ_0) which is equal to 1000 kg/m³ for the SI units used in the current study.

Numerical Methods

Dynamic analysis of airflow in the human nasal cavity is conducted in numerical simulation through a commercial package Fluent. Simulation of flow fields is performed by solving full Navier-Stokes equations. In order to track individual particle behaviour, discrete phase model (DPM) Lagrangian method is used to trace the dispersion of particles about the trajectory. The Lagrangian scheme treats the particle phase as a discrete phase, and the fluid phase as a carrier phase in a Eulerian frame. Trajectories of individual particles can be tracked by balancing the forces acting on them. The Lagrangian scheme is most popular in engineering applications for the prediction of particulate flows because it can easily be combined with a stochastic scheme, albeit with high computational cost. In the Lagrangian model, the fluid phase is solved by Eulerian equations, and then integrates Lagrangian equations of motion for the dispersed phase, tracking individual particles through the flow field

Governing Equations

Under the assumption that the ambient air is incompressible, has constant density and viscosity, and the flow is steady and laminar, the governing equations can be expressed in the following form:

the continuity equation:

$$\nabla \cdot \vec{V} = 0 \quad (1)$$

and the Navier–Stokes equation:

$$\nabla \cdot (\rho \vec{V} \vec{V}) = -\nabla P + \nabla \cdot (\bar{\tau}) + \vec{F} \quad (2)$$

where ρ is the gas density, P the static pressure, $\bar{\tau}$ the stress tensor and \vec{F} the external body force.

The equations are discretized in space using a cell-centered finite volume formulation. The coupling between pressure and velocity is solved using the Semi-Implicit Method for Pressure Linked Equations (SIMPLE) algorithm. Time integration is performed using a fully implicit procedure. The linear system which results is solved using a line Gauss–Seidel (LGS) iterative scheme. A multigrid scheme, which involves four automatic successive coarsenings of the original grid, is used to enhance convergence of the pressure correction equation.

Lagrangian Dispersed Phase Model

The Lagrangian dispersed phase model [14] is used for the prediction of the trajectory of a particle. This is done by integrating the force balance on the particle. The force balance equates the particle inertia with the force acting on the particle, and can be written as:

$$\frac{du_p}{dt} = F_D(u - u_p) + g_x(\rho_p - \rho) / \rho_p + F_x \quad (3)$$

where $F_D(u - u_p)$ is the drag force per unit particle mass and

$$F_D = \frac{18\mu C_D \text{Re}}{\rho_p D_p^2 24} \quad (4)$$

$$\text{Re} = \frac{\rho D_p |u_p - u|}{\mu} \quad (5)$$

The term F_x represents additional forces such as thermophoretic force, Saffman's lift force or virtual mass force. However, provided that the particles meet the condition that $\rho_p > \rho$, these terms can be neglected, except for the force caused by the pressure gradient in the fluid when there are high acceleration forces present:

$$F_x = \left(\frac{\rho}{\rho_p} \right) u_p \frac{\partial u}{\partial x} \quad (6)$$

The term g_x is the gravitational body force. The drag coefficient, C_D is given by:

$$C_D = a_1 + \frac{a_2}{R_e} + \frac{a_3}{R_e^2} \quad (7)$$

where the constants are given by Moris and Alexander [15], and take account of ultra-Stokesian drag.

The momentum transfer from the continuous phase to the particle phase is computed by examining the change in momentum of a particle as it passes through each control volume.

Results and Discussions

Numerical computations are focused on flow behaviour of particle transportation and deposition through the sections, which can be used by pharmaceutical companies and clinicians who need to predict and optimise inhaled therapies.

Particle Transportation through Domain Sections

Particle transportation through the domain section is numerically predicted as shown in Figure 4, which is mainly controlled by particle size and density. It is notice that nasal cavity has a filtering and carrying function depending on different properties of particle. It can be concluded that such numerical simulation can provide the convenient way to optimise various range materials to be inhaled.

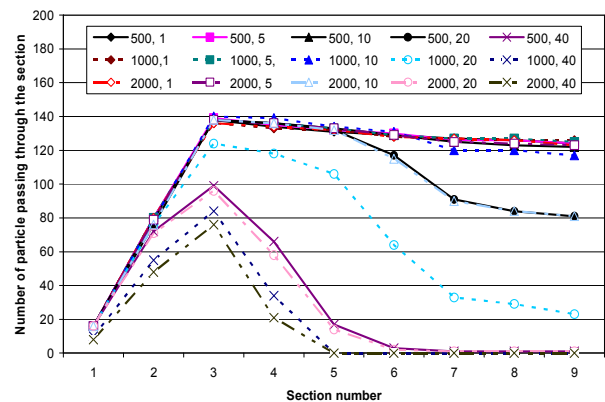
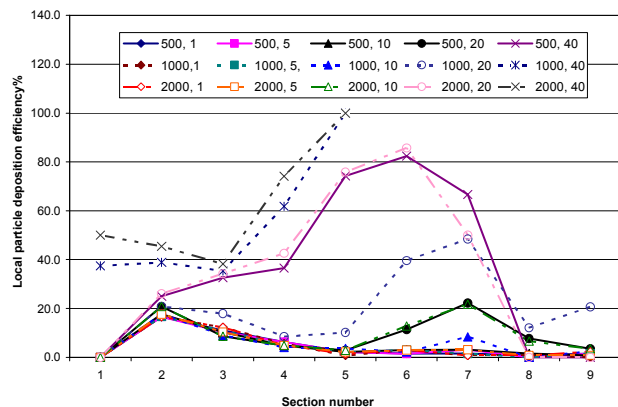


Figure 4. Particle transportation through domain sections at the 125ml/s of airflow rate, comparing with different material properties of particle, e.g. (500, 1) = (density, diameter).

Particle Deposition Efficiency

Particle depositions along the flow channel are shown in Figure 5, a concentration peak is appeared at the middle section for high density particle, the peak move into downstream sections.



Figures 5. Particle deposition efficiency on domain sections at the 125ml/s of airflow rate, comparing with different materials properties of particle, e.g. (500, 1) = (density, diameter).

Comparisons of velocity profiles

Comparison of velocity profile at the section 8 is shown in Figure 6, with previous experimental [8] and computational [11] results.

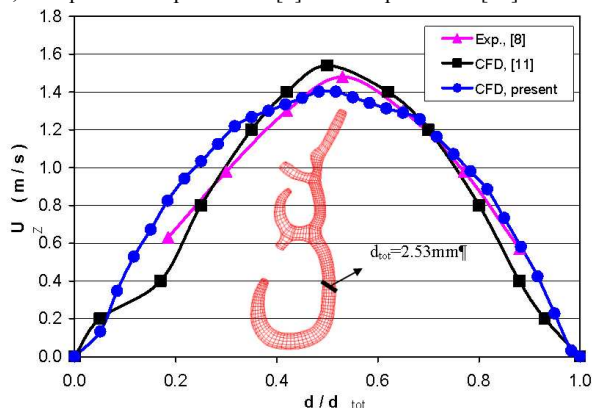


Figure 6. Comparison of velocity profile at the section 8 in Z direction with previous experimental [8] and computational [11] results.

Comparisons of total deposition efficiency

Comparison of total particle deposition efficiency is shown in Figure 7, with previous experimental [16, 17] and calculated [13] results. The discrepancy shown that different approaches are difficult to replicate the nasal flow processes.

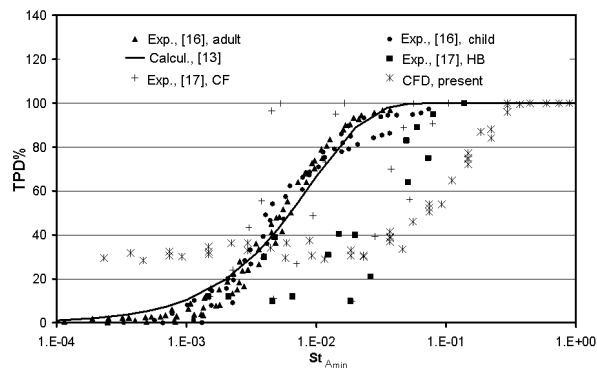


Figure 7. Comparison of total particle deposition efficiency with previous experimental [16, 17] and calculated [13] results.

Conclusions

Airflow features in the human nasal cavity have a strongly influence on the drug delivery process and particle physical

characteristics. Numerical simulation provides the convenient way to optimise various drug materials to be inhaled.

Acknowledgments

The financial support from ARC Linkage grant and RMIT-VRII grant on this work is gratefully acknowledged.

References

- [1] Balashazy, I. and Hofmann, W., Particle Deposition in Airway Bifurcations – I. Inspiratory Flow, *J. Aerosol Sci.*, 1993, **24**, 745-772.
- [2] Yu, G., Xhang, Z. and Lessmann, R., Fluid Flow and Particle Diffusion in the Human Upper Respiratory System, *Aerosol Sci. Technol.*, 1998, **28**, 146-158.
- [3] Zhang, Z., Kleinstreuer, C. and Kim, C. S., Cyclic Micron-Size Inhalation and Deposition in a Triple Bifurcation Lung Airway Model, *J. Aerosol Sci.*, 2002a, **33**, 257-281.
- [4] Zhang, Z., Kleinstreuer, C. and Kim, C. S., Micro-Particle Transport and Deposition in a Human Oral Airway Model, *J. Aerosol Sci.*, 2002b, **33**, 1635-1652.
- [5] Martonen, T. B., Zhang Z., Yue, G., and Musante, C. J., 3-D Particle Transport Within the Human Upper Respiratory Tract, *J. Aerosol Sci.*, 2002, **33**, 1095-1110.
- [6] Gemci, T., Shortall, B., Allen, G.M., Corcoran, T. E. and Chiger, N., A CFD Study of the Throat During Aerosol Drug Delivery Using Heliox and Air, *J. Aerosol Sci.*, 2003, **34**, 1175-1192.
- [7] Matida, E. A., Finlay, W. H., Lange, C. F. and Grgic, B., Improved Numerical Simulation of Aerosol Deposition in an Idealized Mouth-Throat, *J. Aerosol Sci.*, 2002, **35**, 1-19.
- [8] Hahn, I., Scherer, P. W. and Mozell, M. M., Velocity Profiles Measured for Airflow through a Large-scale Model of the Human Nasal Cavity, *Modeling in Physiology*, 1993, **75**, 2273-2287.
- [9] Swift, D. L. and Strong, J. C., Nasal Deposition of Ultrafine ^{218}Po Aerosols in Human Subjects, *J. Aerosol Sci.*, 1996, **27**, 1125-1132.
- [10] Hörschler, I., Meinke, M. and Schröder, W., Numerical Simulation of the Flow Field in a Model of the Nasal Cavity, *Comp. Fluids*, 2003, **32**, 39-45.
- [11] Keyhani, K., Scherer, P.W., and Mozell, M.M. Numerical simulation of airflow in the human nasal cavity. *J. Biomech. Eng.*, 1995, **117**, 429-441.
- [12] Keyhani, K., Scherer, P.W., and Mozell, M.M., A numerical model of nasal odorant transport for the analysis of human olfaction, *J. Theoretical Biology*, 1997, **186**, 279-301.
- [13] Cheng, Y.S. Aerosol Deposition in the Extrathoracic Region. *J. Aerosol Sci. Tech.*, 2003, **37**, 659-671.
- [14] Migdal, D, Agosta, D.V., A source flow model for continuum gas-particle flow, *Trans. ASME J. Appl. Mech.* 1967, 34E 860.
- [15] Morsi, S.A, Alexander, A.J., An investigation of particle trajectories in two-phase flow systems, *J. Fluid Mech.*, 1972; 55: 193-208.
- [16] Swift, D.L., Inspiratory Inertial Deposition of Aerosols in Human Airway Replicate Casts: Implication for the Proposed NCRP Lung model. *Radiat. Prot. Dosim.*, 1991, **38**, 29-34.
- [17] Häußermann, S., Bailey, A.G., Baily, M.R., Etherington, G., and Youngman, M., The influence of breathing patterns on particle deposition in a nasal replicate cast. *J. Aerosol Sci.*, 2002, **33**, 923-933.